Tersedia online di: http://ejournal.undip.ac.id/index.php/teknik

TEKNIK, 43 (1), 2022, 78-86

Analysis of $CaCO_3$ Impregnation on HY Zeolite Surface Area, Pore Size, and Activity in the Catalytic Cracking of Palm Oil to Biofuels

Rosyad Adrian Febriansyar[1], **Teguh Riyanto**[1,2], **I. Istadi**[1,2,*]

[1] *Department of Chemical Engineering, Faculty of Engineering, Universitas Diponegoro,*
Semarang 50275, Indonesia.
[2] *Laboratory of Plasma-Catalysis (R3.5), Center of Research and Services - Diponegoro University (CORES-DU),*
Integrated Laboratory, Universitas Diponegoro, Semarang, Central Java 50275, Indonesia

Abstract

Fossil energy sources are currently decreasing, requiring the development of alternative energy sources. Vegetable oil is a raw material for alternative renewable energy supplies. This study produced biofuels from vegetable oil using calcium carbonate ($CaCO_3$)-impregnated HY catalysts. In addition, this study aimed to investigate the effect of $CaCO_3$ impregnation on the surface area and the catalytic activity of catalysts in the palm oil cracking process to produce biofuels. The HY catalyst was modified by the wet impregnation method in 5 wt% $CaCO_3$ solution and was further calcined at 550°C for three h. Furthermore, the catalysts were tested in a continuous fixed-bed catalytic reactor at 450°C. The catalyst properties were characterized using Brunauer–Emmett–Teller (BET) surface area, Barrett–Joyner–Halenda (BJH) for pore size distribution, and X-Ray Diffraction (XRD) for crystal structure and phases. The results showed that the addition of $CaCO_3$ decreased surface area and pore volume; however, the pore size increased, which resulted in the production of heavy hydrocarbons. Interestingly, the introduction of $CaCO_3$ enhanced the yield of Organic Liquid Product (OLP) and diesel-range hydrocarbons selectivity to reach 79.09% and 30.54%, respectively. Furthermore, the introduction of $CaCO_3$ increased deoxygenation activity.

Keywords*: Catalyst activity, biofuel, calcium carbonate, deoxygenation*

1. Introduction

The fast growth of the population and economy in contemporary civilization affects the energy demand, which continues to increase constantly. Whilst fossil fuels have usually been the primary source of energy, their supply is very restricted and continues to decrease (Sharma & Sheth, 2015). When fossil fuels are utilized indefinitely, they have a significantly detrimental influence on the environment. With rising energy demand and diminishing fossil fuel reserves, it is critical to develop renewable energy sources to satisfy energy demands. Since biofuels are renewable energy sources, palm oil (biofuel) offers enormous potential to satisfy energy demands (Riyanto *et al*., 2020)

Biofuels have been discovered to have a high potential for usage as a fossil fuel alternative. Biofuels, including gaseous and liquid fuels, are often derived from renewable resources. Gaseous biofuels, such as methane and hydrogen, and liquid biofuels, like biogasoline and biodiesel, are the primary energy sources for automobiles and other vehicles. Moreover, it can be utilized to generate power (Ahmad *et al*., 2016). Plant oils, such as vegetable oils and palm oil, mainly comprise triglycerides and can be easily converted into liquid biofuels (Twaiq *et al*., 2004).

Palm oil is an alternative feedstock for biofuel (Ndayishimiye & Tazerout, 2011). Its physical and chemical properties are very similar to that of diesel. However, due to its high viscosity, its direct use as a fuel in diesel engines can cause poor atomization, carbon deposition, or blockage of the fuel lines. It is necessary to convert palm oil into alternative fuels to replace the existing fossil fuels. At present, catalytic cracking is required to lower the acid value and oxygen content of biofuels to enhance fuel attributes such as density, calorific value, and dynamic viscosity. Catalysts are used to break down lipids to produce biofuels (Zheng, Lei, *et al*., 2019). Several studies have been conducted to convert vegetable oil into hydrocarbons, namely Pyrolysis (Nomura & Terwilliger, 2019), transesterification (Thaoklua *et al*., 2018), and catalytic

---

[*] Corresponding Author.
E-mail: istadi@che.undip.ac.id

doi: 10.14710/teknik.v43i1.44579

cracking (Doronin *et al*., 2013). Catalytic cracking is the most advanced method for converting vegetable oils to biofuels owing to its low energy needs, low operating costs, and great flexibility in using a variety of vegetable oils (Istadi *et al*., 2020).

Various solid catalysts for biofuel production have been developed, including alkaline bases, zeolites, and modified zeolites (Kesić *et al*., 2012). In the case of catalytic cracking, the most developed base catalysts were CaO-based catalysts, while the most developed acid catalysts were zeolite-based catalysts (Riyanto *et al*., 2020). An appropriate catalyst must be developed for biofuel production through catalytic cracking of palm oil. The properties of the employed catalyst are critical in synthesizing biofuels from palm oil (Istadi *et al*., 2020).

Commercial synthetic zeolites are more often utilized than natural zeolites due to their greater purity and particle size uniformity, making them more suitable for most scientific applications and purposes (Z. Liu *et al*., 2016). CaO catalyst can be obtained from the decomposition of $CaCO_3$, which affects the crystal structure, surface area, and pore size (Zul *et al*., 2021). According to Nurjannah *et al*. (2012), at 450°C, the palm oil cracking process over HZSM-5 catalyst yields gasoline, kerosene, and diesel of 28.78%, 16.57%, and 7.65%, respectively. Based on the research conducted by Yi *et al*. (2019), the addition of CaO in the cracking process produced more BTX (Benzene, Toluene, Xylene). According to Yan *et al*. (2008), the CaO supported by zeolite catalyst has the maximum activity compared to catalysts MgO that were not supported by zeolite catalyst. In the other report, the production of CaO from the calcination of $CaCO_3$ resulted in a higher fuel yield (Chireshe *et al*., 2020). Research conducted by Istadi *et al*. (2021), the surface area of the Ni-modified HY catalyst is decreased. However, there was an increase in OLP yield and selectivity in the catalytic cracking process. Yigezu & Muthukumar (2014) reported that the surface area affects the catalysts' performance in the catalytic cracking process.

According to the previous studies, adding $CaCO_3$ to zeolite HZSM-5 could improve the catalyst's activity because reducing the surface area enhances gasoline conversion and heavy hydrocarbons by 99.65% and 38.65%, respectively (Kianfar *et al*., 2018). Based on previous research, the study on the effect of $CaCO_3$ impregnation on HY zeolite on surface area and pore size of catalysts for palm oil cracking is relatively restricted. In addition, the effect of $CaCO_3$ impregnation to HY zeolite on the catalysts' surface area and pore properties is also important since the catalyst is one of the important properties in catalytic cracking. Therefore, this research aims to evaluate the impact of $CaCO_3$ addition on catalysts' surface area, pore size, and catalytic activity throughout the conversion process.

Table 1. Fatty acids composition of palm oil (Istadi *et al*., 2021)

No	Component	Composition (%)
1.	Palmitic acid (C16:0)	44.53
2.	Stearic acid (C18:0)	1.80
3.	Oleic acid (C18:1)	41.91
4.	1-Tridecene	5.32
5.	2,6,10,14,18-Penta Methyl Eicosa pentane	6.44
	Total	**100.00**

2. Materials and Methods

2.1. Materials

This study used HY-zeolite catalyst material, obtained commercially from Zeolyst International as CBV760, and calcium carbonate ($CaCO_3$) (99.0%, Merck) as a precursor. As the feedstock, palm oil was obtained from the local market in Semarang. The specifications for palm oil can be seen in Table 1. In addition, Nitrogen gas (99% UHP) from PT. Samator was also used in this study to remove/flush oxygen content inside the pipelines and reactor instruments.

2.2. Catalysts' preparation

Zeolite HY was dried for 1 hour at 110 °C in an electric oven (Memmert) and labeled as HY. Then, 20 g of HY was immersed in a 75mL $CaCO_3$ solution (0.25 M) so that the impregnated $CaCO_3$ was 5 wt% on the HY-zeolite catalyst. The slurry was stirred at a stirring speed of 600 rpm for 1 hour. After that, the slurry was aged for 12 hours. The mixture was then filtered and dried for 12 hours at a temperature of 65°C in an electric oven (Memmert). The catalyst was then calcined at 550 °C for 3 hours in a furnace (ThermoLyne) and labeled as $CaCO_3$/HY catalyst.

2.3. Catalysts' characterization

The crystal structure of the catalysts was determined using X-ray diffraction (XRD) analysis (Shimadzu 7000) at 30 kV and 30 mA in the presence of Cu-Kα radiation. With a scanning speed of 3°/min, the catalyst was scanned at an angle of 2θ 5-90°. The adsorption-desorption of N_2 is a tool to identify a catalyst's surface area and pore size distribution. The surface area of the catalyst was determined using the Braunauer-Emmett-Teller (BET) technique. At the same time, the Barret-Joyner-Halenda (BJH) technique was used to determine the pore size distribution. The BET and BJH techniques are estimated using N_2 gas adsorption at -196°C (Tsai, 2013).

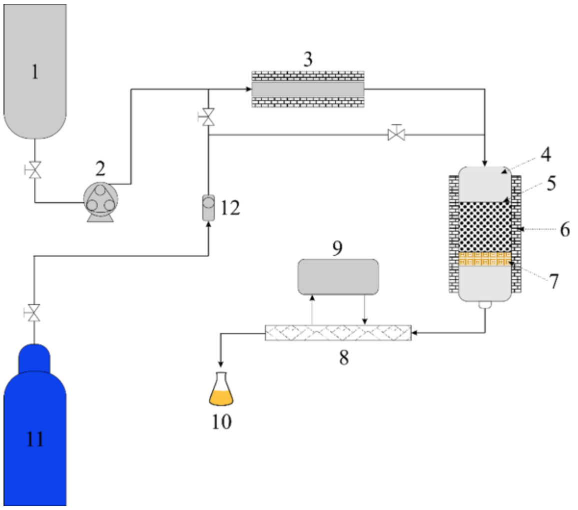

Figure 1. Scheme of the catalytic cracking rig: 1) Palm oil tank, 2) Peristaltic pump, 3) Pre-Heater, 4) Fixed-bed reactor, 5) Catalyst bed, 6) Electric heater, 7) Glass wool, 8) Condensor, 9) Water-cooler, 10) Organic liquid product, 11) N_2 gas tank, 12) Flowmeter

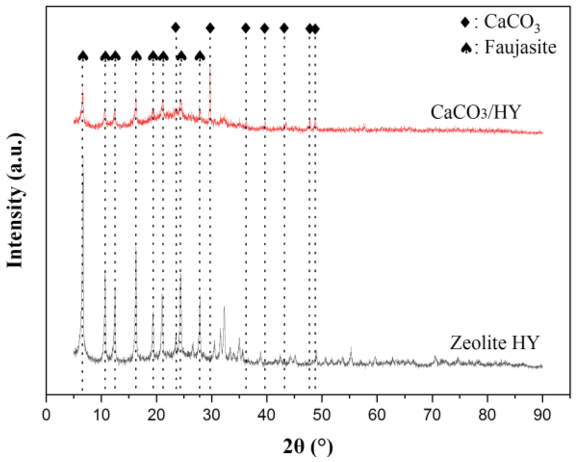

Figure 2. X-ray diffraction pattern of HY and $CaCO_3$/HY catalysts

2.4. Catalyst performance testing and biofuel analysis

The catalysts were tested for their catalytic performances for the cracking of palm oil using a fixed-bed catalytic reactor (Figure 1) to produce liquid fuels. The reactor was constructed with a stainless-steel tube with a diameter of 1 inch. A 450°C electric heating furnace is installed before the reactor as a pre-heater. Five grams HY and $CaCO_3$/HY catalysts were introduced into the reactor. Then, for 15 minutes, 100 mL/min of N_2 gas was flowed into the experimental apparatus to ensure no oxygen was connected to the stainless-steel surface. The reactor was heated until stable at the temperature reached 450°C. Thus, palm oil was fed into the reactor at a weight hourly space velocity (WHSV) of 0.288/min. A peristaltic pump (RZ1030-BX) controls the flow rate. The first 30 minutes were spent establishing the steady-state condition for the catalytic cracking process. Then, for four hours, the cracking process began. The product is condensed into an organic liquid product (OLP) after the cracking process. The non-condensable product and coke were classified as the by-products of the cracking process.

The organic liquid product (OLP), as a crude hydrocarbon and oxygenates product, was condensed and distilled fractionally based on ASTM D-86. The temperature range of gasoline range 39-204ºC (CAS 86290-81-5), kerosene range 204-300ºC (CAS 8008-20-6), and diesel range 300-370ºC (CAS 68334-30-5). The yield and selectivity were calculated based on Equations (1)-(5).

$$Yield\ of\ OLP(\%) = \frac{m_{OLP}}{m_{feed}} x100 \tag{1}$$

$$Yield\ of\ gas(\%) = \frac{m_{OLP}}{m_{feed}} x100 \tag{2}$$

$$Yield\ of\ coke(\%) = \frac{m_{coke}}{m_{feed}} x100 \tag{3}$$

$$Yield\ of\ water(\%) = \frac{m_{water}}{m_{feed}} x100 \tag{4}$$

$$Selectivity\ of\ diesel = \frac{m_{diesel}}{m_{OLP}} x100 \tag{5}$$

3. Result and Discussion

3.1. X-Ray Diffraction (XRD) Analysis on the Catalysts

The synthesized catalysts were characterized by diffraction patterns using XRD analysis to identify the crystal structure of HY and $CaCO_3$/HY catalysts. Sharp peaks in the diffraction pattern suggest a crystalline structure, while broad peaks indicate an amorphous structure (Zhou & Chen, 2016). In Figure 2, the resulting diffraction peaks were matched with the JCPDS (Joint Committee on Powder Diffraction Standards) presented in Table 2.

Figure 2 shows the diffraction pattern of the HY catalyst (Faujasite). There are five sharp diffractions

Table 2. JCPDS compound data for HY and $CaCO_3$/HY catalysts

Data	**Compound**	**2θ**						
JCPDS File	$CaCO_3$[a]	23	29.4	35.5	39.4	43.1	47.5	48.5
	Faujasite[b]	6.2	10.1	11.8	15.6	23.5	-	-
HY	Faujasite	6.6	10.6	12.4	16.2	24.3	-	-
$CaCO_3$/HY	$CaCO_3$	23.3	29.7	36.2	39.6	43.4	47.7	48.7
	Faujasite	6.6	10.6	12.4	16.2	24.3	-	-

[a] JCPDS no. 72-1651
[b] JCPDS no. 26-0893

with high crystallinity at angles of 2θ = 6.6°, 10.6°, 12.4°, 16.2°, and 24.3°, which is similar to the results similar observation reported by Doyle *et al*. (2016) that HY zeolite has the same angle of 2θ. In this study, those peaks were observed in both catalysts HY and $CaCO_3$/HY catalysts, indicating that the Faujasite structure was present in both catalysts. The diffraction pattern of $CaCO_3$ has seven sharp diffractions shown at angles of 2θ = 23.3°, 29.7°, 36.2°, 39.6°, 43.4°, 47.7°, and 48.7°. The appearance of these diffractions indicates that the $CaCO_3$ has been successfully attached to HY zeolite.

As shown in Figure 2, the diffraction peaks of CaO were not observed in the $CaCO_3$/HY catalyst, indicating that the $CaCO_3$ was not converted to CaO during the calcination process. Research conducted by Lesbani *et al*. (2013) on the decomposition process of $CaCO_3$ with a decomposition temperature of 600°C showed that the decomposition of the compounds had not been completed and required higher temperatures to convert all these compounds into the form of CaO. When increasing the calcination temperature, the diffraction pattern becomes more intense and sharp, indicating a rise in the material's crystallinity and the elimination of $CaCO_3$ (Da Silva Castro *et al*., 2019).

3.2. Physical Properties of Catalysts

The Brauner, Emmet, and Teller (BET) method determined the specific surface area, while the pore size distribution was determined by the Barrett–Joyner–Halenda (BJH) method. The N_2 adsorption-desorption of HY and $CaCO_3$/HY catalysts have been carried out to determine the specific surface area, pore size distribution, total pore volume, and pore structure of the material (Purnamasari *et al*., 2017). Table 3 provides the result of the characterization of the catalysts' surface area, pore-volume, and pore size.

Table 3. Characterization of surface area, pore volume, and pore size of the $CaCO_3$/HY zeolite catalyst in comparison to HY

Catalysts	**Surface area[a] (m^2/g)**	**Pore Volume[b] (cm^3/g)**	**Pore Size[b] (nm)**
HY	686.85	0.491	2.86
$CaCO_3$/HY	298.99	0.362	4.85

[a]BET Method
[b]BJH method

Table 3 shows that the addition of $CaCO_3$ to HY zeolite decreased the surface area and pore volume decreased by 298.99 cm^2/g and 0.362 cm^3/g, respectively. The decrease in pore volume was caused by the pore filling, which was possibly the micropores, by $CaCO_3$. Due to the $CaCO_3$ impregnation, the pore volume and surface area reduced as the micropores were filled or blocked. The supported catalyst is essential in stabilizing the formed metal species during the calcination. However, agglomeration of metals could occur, attaching to the surface of the catalyst (L. Liu & Corma, 2018). Previously, Wang *et al*. (2020) found that the addition of $CaCO_3$ decreased the catalyst's surface area and pore volume, which is similar to this study.

As shown in Figure 3(a), the average pore size of HY catalyst is 2.86 nm, while the $CaCO_3$/HY catalyst is 4.85 nm. This indicates that the impregnation of $CaCO_3$ on HY catalyst increases the average pore size of catalysts. This is due to the addition of calcium carbonate producing more mesopore (Ferrero *et al*., 2015), while Cheng *et al*. (2021) found that the increase average pore size could be controlled by adjusting the concentration of calcium carbonate. In addition, these results indicate that the pore size distribution of the HY and $CaCO_3$/HY catalysts is mesopore. Figure 3(b) shows a type IV isotherm profile of N_2 adsorption-desorption. In the mesopores, the isotherms show capillary condensation and absorption limitations above a certain point in the P/Po ratio (Fathi *et al*., 2014; Friedrich *et al*., 2010). The catalyst's pore size distribution is classified as mesopore (2-50 nm) (Zheng *et al*., 2019). As a result, with the addition of $CaCO_3$, the micropores of $CaCO_3$/HY catalyst are blocked. Thus, the surface area catalyst was decreased. Cheng *et al*. (2021) reported that the pore size distribution could be controlled by adding $CaCO_3$.

3.3. Effect of Catalyst on Yield of Product

In this study, HY and $CaCO_3$/HY catalysts were investigated in the catalytic cracking of palm oil in a fixed bed catalytic reactor to produce the organic liquid

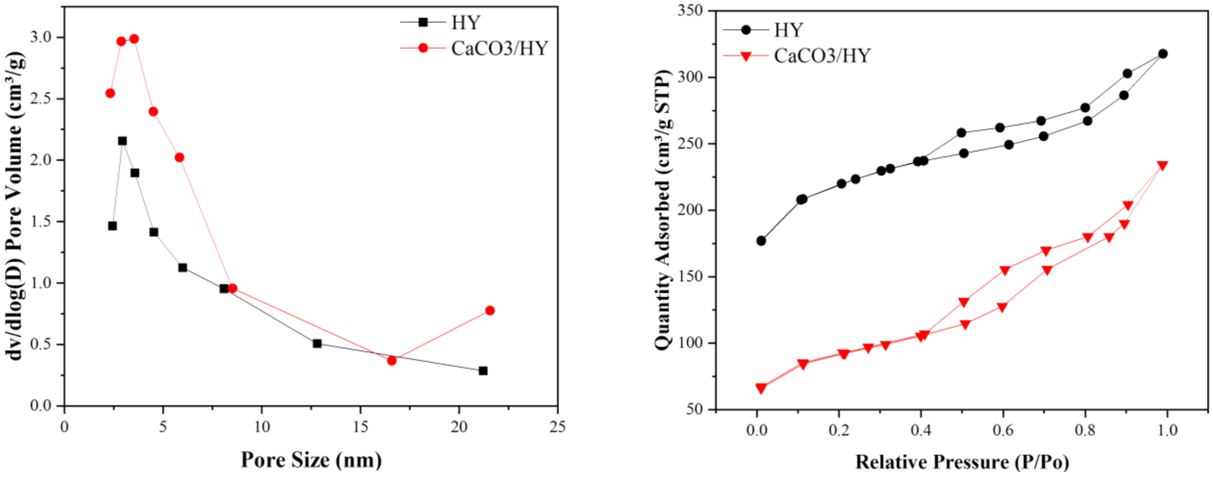

(a)

(b)

Figure 3. (a) pore size distributions and (b) N_2 adsorption-desorption isotherm

product (OLP). The OLP yield was calculated using (Eqs. (1)-(4)).

As shown in Figure 4, $CaCO_3$ increases the production of OLP and coke by 79.09 % and 2.39 %, respectively. The $CaCO_3$ aggregates covering the catalyst surface contributed to the increase in coke yield, which is proven by the BJH result (Table 3). Kianfar *et al*. (2018) suggested that the decrease in the surface area caused by increasing $CaCO_3$ concentration was a factor in the increased production of heavier hydrocarbons. The decrease in surface area is due to the $CaCO_3$ crystals blocking the catalyst pores as found by Zhao *et al*. (2015) that surface area catalysts decrease, leading to increased coke products and a decrease in biofuel products.

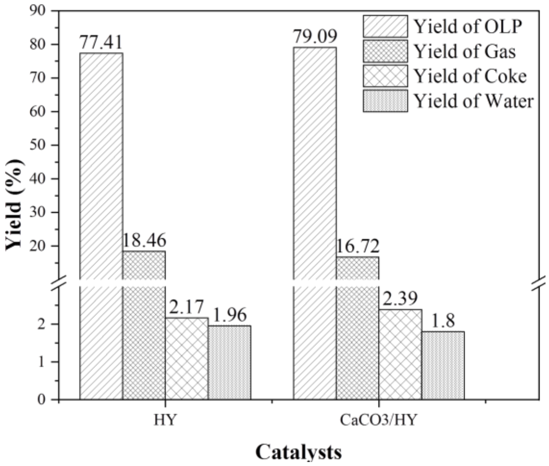

Figure 4. Effect of HY and $CaCO_3$/HY catalysts on product yield

Additionally, the yield of gas and water decreased by 16.72% and 1.80%, respectively, because $CaCO_3$/HY has a lower surface area than HY. Thus, the primary reason for the increase in OLP yield is the mesopore structure of the $CaCO_3$/HY catalyst. The decrease in the yield of gas leads to the formation of heavy hydrocarbons due to the larger pore size, as seen in Table 3. As shown in Figure 4, water was produced through the deoxygenation pathway. Since each catalyst produces water, it is possible to suggest that both catalysts promote the deoxygenation reaction by releasing water molecules.

3.4. Effect of Catalyst on Diesel Selectivity

The catalytic activity performance of HY and $CaCO_3$/HY catalysts was also identified through their product selectivity, especially for the diesel fraction product in Figure 5, which was calculated using Eq. (5). As shown in Figure 5, the addition of $CaCO_3$ increases diesel selectivity by 30.54 %. The addition of $CaCO_3$ to the HY catalyst significantly improves selectivity, which means the $CaCO_3$/HY catalyst may have two catalyst characteristics, acidity, and basicity. Thus, the acidity helps increase diesel selectivity, and basicity helps the deoxygenation process. Verdoliva *et al*. (2019) found that HY zeolite has high acidity characteristics, while Wang *et al*. (2020) found that the addition of $CaCO_3$ can increase the basicity on the catalyst's surface. However, the acidity and basicity characteristics of catalysts will be done further and published elsewhere.

Table 4 . Comparison of previous research on the cracking of palm oil into biofuel

Catalyst	Temperature (°C)	Yield OLP (%)	Selectivity (%)			Reference
			Gasoline	Kerosene	Diesel	
Na_2CO_3	450	68	21	n.a.	66	(Weber *et al*., 2012)
ZSM-5	450	68	69.77	9.51	5.04	(Riyanto *et al*., 2021)
CaO	450	29	40	8.5	16	(Hu *et al*., 2019)
Ni/HY	410	46.3	69		19	(T. Li *et al*., 2016)
Co-CaO	350	64	78	n.a.	34	(Asikin-Mijan *et al*., 2016)
HY	450	77.41	n.a.	n.a.	28.40	This study
$CaCO_3$/HY	450	79.09	n.a.	n.a.	30.54	This study

*n.a : not available

Research by Fathi *et al*. (2014) found that the addition of $CaCO_3$ to the zeolite HSZM-5 enhanced its selectivity. The shape and porosity of the zeolite, on the other hand, influence the selectivity and composition of biofuels (Amalia *et al*., 2021). The increase in selectivity over the $CaCO_3$/HY catalyst occurred due to increased pore size, as shown in Table 3. The increase in $CaCO_3$ concentration resulted in increased catalyst-reactant interactions. The addition of catalyst supports may enhance the catalyst's interaction with the triglyceride molecules (Pasupulety *et al*., 2013). H. Wang *et al*. (2019) explained that catalyst support strongly impacted the triglyceride composition.

As a result, the catalyst's active site may improve diesel selectivity. The absence of gasoline and kerosene may be due to mesopore distribution. The decrease in the surface area (Table 3) caused by increasing $CaCO_3$ concentration was a factor in the increased production of heavier hydrocarbons (Kianfar *et al*., 2018). Peng *et al*. (2015) found that the increase in diesel selectivity was due to mesopore distribution in the catalyst. Catalytic activity usually rises as the active site increases. Moreover, mesoporous zeolite as a replacement for microporous zeolite significantly increased the selectivity toward heavy hydrocarbons (Zhang *et al*., 2014).

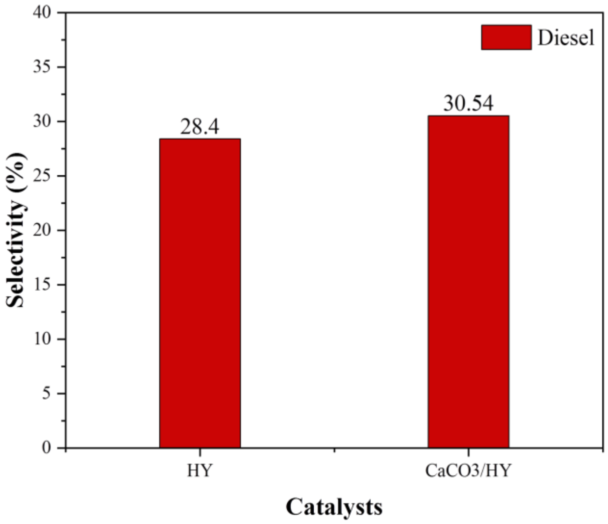

Figure 5. Effect of HY and $CaCO_3$/HY catalyst on diesel selectivity

As can be seen in Figure 5, it is obtained that $CaCO_3$/HY catalyst gives a higher diesel selectivity than HY catalyst. Based on the catalyst characterization, this phenomenon is in line with the pore properties of catalysts. As shown in Table 3 and Figure 3, $CaCO_3$/HY has a larger pore size than HY catalyst. The pore size of the $CaCO_3$/HY catalyst is near twice that of HY pore size. Therefore, it can be suggested that the different selectivity of diesel is due to the pore shape-size-selectivity of zeolite. It was also previously postulated that pore structure could affect the catalyst activity in cracking reaction (Jung *et al*., 2004; S. C. Li *et al*., 2021). As the pore size is large enough, the cracking product can be easily released from the surface. It is true since it was reported that the cracking product could be trapped in micropores because of diffusion limitation (S. C. Li *et al*., 2021). Furthermore, the synthesized catalysts in this study have better activity than in some previous studies, as shown in Table 4.

Table 4 shows that the $CaCO_3$/HY catalyst obtained better results than in previous studies. The yield of OLP produced in this study is high enough. In addition, the HY and $CaCO_3$/HY strongly confirmed that catalysts show the highest diesel selectivity but are not adequate for gasoline and kerosene production. Additionally, adding 5%wt $CaCO_3$ into HY can increase catalyst activity to produce diesel fractions. It is due to the $CaCO_3$/HY having large pore sizes that can release the cracking product as long-chain hydrocarbons due to the pore selectivity. Moreover, the $CaCO_3$/HY catalyst has a higher diesel selectivity than HY catalyst due to the pore selectivity since $CaCO_3$/HY has a larger pore size than HY catalyst. Therefore, it can be concluded that the addition of $CaCO_3$ to HY catalyst could increase the pore size, leading to the formation of long-chain hydrocarbons.

4. Conclusion

Adding 5wt% $CaCO_3$ to the HY catalyst made a significant impact on decreasing surface area and pore volume and enhancing pore size. These concentrations resulted in a decrease in surface area and pore volume due to the micropore blocking by $CaCO_3$. However, the pore size increased because the micropore was blocked by $CaCO_3$, leaving the mesopore. The experimental data of HY and $CaCO_3$/HY catalysts showed that the yield of OLP increased from 77.41% to 79.09%. On the other hand, the yield of gas, coke, and water decreased from 18.46% to 16.72%, 2.17% to 2.39%, and 1.96% to 1.8%, respectively. The presence of water in each catalyst indicates a deoxygenation reaction in the catalytic cracking process. Furthermore, there was an improvement in diesel selectivity of 30.54% by using $CaCO_3$/HY catalyst in catalytic cracking of palm oil using a fixed-bed catalytic reactor. These findings are essential for the future development of catalysts. Further improvements in biofuels production using $CaCO_3$/HY catalyst can be achieved by optimizing the concentration of $CaCO_3$ as the catalysts' active site.

Acknowledgment

The authors would like to express their sincere gratitude to Research Institution and Community Service, Universitas Diponegoro, Indonesia, for the financial support through the World Class Research Universitas Diponegoro (WCRU) research project category A with contract number: 118-22/UN7.6.1/PP/2021.

References

Ahmad, M., Farhana, R., Raman, A. A. A., & Bhargava, S. K. (2016). Synthesis and activity evaluation of heterometallic nano oxides integrated ZSM-5 catalysts for palm oil cracking to produce biogasoline. *Energy Conversion and Management*, *119*, 352–360. https://doi.org/10.1016/j.enconman.2016.04.069

Amalia, R., Riyanto, T., & Istadi, I. (2021). Reactivation of the Spent Residue Fluid Catalytic Cracking (RFCC) Catalyst through Acid Treatment for Palm Oil Cracking to Biofuels. *Teknik*, *42*(2), 218–225. https://doi.org/10.14710/teknik.v42i2.39642

Asikin-Mijan, N., Lee, H. V., Juan, J. C., Noorsaadah, A. R., Abdulkareem-Alsultan, G., Arumugam, M., & Taufiq-Yap, Y. H. (2016). Waste clamshell-derived CaO supported Co and W catalysts for renewable fuels production via cracking-deoxygenation of triolein. *Journal of Analytical and Applied Pyrolysis*, *120*, 110–120. https://doi.org/10.1016/j.jaap.2016.04.015

Cheng, H., Zhang, J., Chen, Y., Zhang, W., Ji, R., Song, Y., Li, W., Bian, Y., Jiang, X., Xue, J., & Han, J. (2021). Hierarchical porous biochars with controlled pore structures derived from co-pyrolysis of potassium/calcium carbonate with cotton straw for efficient sorption of diethyl phthalate from aqueous solution. *Bioresource Technology*, *346*(8), 126604. https://doi.org/10.1016/j.biortech.2021.126604

Chireshe, F., Collard, F. X., & Görgens, J. F. (2020). Production of an upgraded bio-oil with minimal water content by catalytic Pyrolysis: Optimisation and comparison of CaO and MgO performances. *Journal of Analytical and Applied Pyrolysis*, *146*(December 2019), 104751. https://doi.org/10.1016/j.jaap.2019.104751

Da Silva Castro, L., Barañano, A. G., Pinheiro, C. J. G., Menini, L., & Pinheiro, P. F. (2019). Biodiesel production from cotton oil using heterogeneous CaO catalysts from eggshells prepared at different calcination temperatures. *Green Processing and Synthesis*, *8*(1), 235–244. https://doi.org/10.1515/gps-2018-0076

Doronin, V. P., Potapenko, O. V., Lipin, P. V., & Sorokina, T. P. (2013). Catalytic cracking of vegetable oils and vacuum gas oil. *Fuel*, *106*, 757–765. https://doi.org/10.1016/j.fuel.2012.11.027

Doyle, A. M., Albayati, T. M., Abbas, A. S., & Alismaeel, Z. T. (2016). Biodiesel production by esterification of oleic acid over zeolite Y prepared from kaolin. *Renewable Energy*, *97*, 19–23. https://doi.org/10.1016/j.renene.2016.05.067

Fathi, S., Sohrabi, M., & Falamaki, C. (2014). Improvement of HZSM-5 performance by alkaline treatments : Comparative catalytic study in the MTG reactions. *FUEL*, *116*, 529–537. https://doi.org/10.1016/j.fuel.2013.08.036

Ferrero, G. A., Sevilla, M., & Fuertes, A. B. (2015). Mesoporous carbons synthesized by direct carbonization of citrate salts for use as high-performance capacitors. *Carbon*, *88*, 239–251. https://doi.org/10.1016/j.carbon.2015.03.014

Friedrich, H., Jongh, P. E. De, Bulut, M., Donk, S. Van, Kenmogne, R., Finiels, A., Hulea, V., & Fajula, F. (2010). Zeolite Y Crystals with Trimodal Porosity as Ideal Hydrocracking. *Angewandte Chemie International Edition*, *49*(52), 10074–10078.

https://doi.org/10.1002/anie.201004360

Hu, W., Wang, H., Lin, H., Zheng, Y., Ng, S., Shi, M., Zhao, Y., & Xu, R. (2019). Catalytic decomposition of oleic acid to fuels and chemicals: Roles of catalyst acidity and basicity on product distribution and reaction pathways. *Catalysts*, *9*(12). https://doi.org/10.3390/catal9121063

Istadi, I., Riyanto, T., Buchori, L., Anggoro, D. D., Gilbert, G., Meiranti, K. A., & Khofiyanida, E. (2020). Enhancing Brønsted and Lewis Acid Sites of the Utilized Spent RFCC Catalyst Waste for the Continuous Cracking Process of Palm Oil to Biofuels. *Industrial and Engineering Chemistry Research*, *59*(20), 9459–9468. https://doi.org/10.1021/acs.iecr.0c01061

Istadi, I., Riyanto, T., Buchori, L., Anggoro, D. D., Pakpahan, A. W. S., & Pakpahan, A. J. (2021). Biofuels Production from Catalytic Cracking of Palm Oil Using Modified HY Zeolite Catalysts over A Continuous Fixed Bed Catalytic Reactor. *International Journal of Renewable Energy Development*, *10*(1), 149–156. https://doi.org/10.14170/ijred.2021.33281

Jung, J. S., Kim, T. J., & Seo, G. (2004). Catalytic cracking of n-octane over zeolites with different pore structures and acidities. *Korean Journal of Chemical Engineering*, *21*(4), 777–781. https://doi.org/10.1007/BF02705520

Kesić, Ž., Lukić, I., Brkić, D., Rogan, J., Zdujić, M., Liu, H., & Skala, D. (2012). Mechanochemical preparation and characterization of CaO·ZnO used as catalyst for biodiesel synthesis. *Applied Catalysis A: General Jo*, *427–428*, 58–65. https://doi.org/10.1016/j.apcata.2012.03.032

Kianfar, E., Salimi, M., Pirouzfar, V., & Koohestani, B. B. (2018). Synthesis and modification of zeolite ZSM-5 catalyst with solutions of calcium carbonate (CaCO3) and Sodium Carbonate (Na2CO3) for Methanol to Gasoline Conversion. *International Journal of Chemical Reactor Engineering*, *16*(7), 1–7. https://doi.org/10.1515/ijcre-2017-0229

Lesbani, A., Tamba, P., Mohadi, R., & Fahmariyanti. (2013). Preparation of calcium oxide from Achatina fulica as catalyst for production of biodiesel from waste cooking oil. *Indonesian Journal of Chemistry*, *13*(2), 176–180. https://doi.org/10.22146/ijc.21302

Li, S. C., Lin, Y. C., & Li, Y. P. (2021). Understanding the catalytic activity of microporous and mesoporous zeolites in cracking by experiments and simulations. *Catalysts*, *11*(9), 1–13. https://doi.org/10.3390/catal11091114

Li, T., Cheng, J., Huang, R., Yang, W., Zhou, J., & Cen, K. (2016). Hydrocracking of palm oil to jet biofuel over different zeolites. *International Journal of Hydrogen Energy*, *41*(47), 21883–21887. https://doi.org/10.1016/j.ijhydene.2016.09.013

Liu, L., & Corma, A. (2018). Metal Catalysts for Heterogeneous Catalysis: From Single Atoms to Nanoclusters and Nanoparticles [Review-article]. *Chemical Reviews*, *118*(10), 4981–5079. https://doi.org/10.1021/acs.chemrev.7b00776

Liu, Z., Shi, C., Wu, D., He, S., & Ren, B. (2016). A Simple Method of Preparation of High Silica Zeolite y and Its Performance in the Catalytic Cracking of Cumene. *Journal of Nanotechnology*, *2016*. https://doi.org/10.1155/2016/1486107

Ndayishimiye, P., & Tazerout, M. (2011). Use of palm oil-based biofuel in the internal combustion engines: Performance and emissions characteristics. *Energy*, *36*(3), 1790–1796. https://doi.org/10.1016/j.energy.2010.12.046

Nomura, K., & Terwilliger, P. (2019). Self-dual Leonard pairs Pyrolysis of palm oil using zeolite catalyst and characterization of the boil-oil. *Green Process Synth*, *8*, 649–658.

Nurjannah, Roesyadi, A., & Prajitno, D. H. (2012). Konversi Katalitik Minyak Sawit Untuk Menghasilkan Biofuel Menggunakan Silika Alumina Dan HZSM-5 Sintesis. *Reaktor*, *13*(1), 37–43. https://doi.org/10.14710/reaktor.13.1.37-43

Pasupulety, N., Gunda, K., Liu, Y., Rempel, G. L., & Ng, F. T. T. (2013). Production of biodiesel from soybean oil on CaO/Al2O3 solid base catalysts. *Applied Catalysis A: General*, *452*, 189–202. https://doi.org/10.1016/j.apcata.2012.10.006

Peng, X., Cheng, K., Kang, J., Gu, B., Yu, X., Zhang, Q., & Wang, Y. (2015). Impact of Hydrogenolysis on the Selectivity of the Fischer – Tropsch Synthesis : Diesel Fuel Production over Mesoporous Zeolite Y- Supported Cobalt Nanoparticles **. *Heterogeneous Catalysis*, *54*, 1–5. https://doi.org/10.1002/anie.201411708

Purnamasari, A. P., Sari, M. E. F., Kusumaningtyas, D. T., Suprapto, S., Hamid, A., & Prasetyoko, D. (2017). The effect of mesoporous H-ZSM-5 crystallinity as a CaO support on the transesterification of used cooking oil. *Bulletin of Chemical Reaction Engineering & Catalysis*, *12*(3), 329–336. https://doi.org/10.9767/bcrec.12.3.802.329-336

Riyanto, T., Istadi, I., Buchori, L., Anggoro, D. D., & Dani Nandiyanto, A. B. (2020). Plasma-Assisted Catalytic Cracking as an Advanced Process for Vegetable Oils Conversion to Biofuels: A Mini Review. *Industrial & Engineering Chemistry Research*, *59*(40), 17632–17652. https://doi.org/10.1021/acs.iecr.0c03253

Riyanto, T., Istadi, I., Jongsomjit, B., Anggoro, D. D., Pratama, A. A., & Al Faris, M. A. (2021). Improved Brønsted to Lewis (B/L) Ratio of Co- and Mo-Impregnated ZSM-5 Catalysts for Palm Oil Conversion to Hydrocarbon-Rich Biofuels. *Catalysts*, *11*(1286), 1–14.

Sharma, R., & Sheth, P. N. (2015). Thermo-Chemical Conversion of Jatropha Deoiled Cake : Pyrolysis vs. Gasification. *International Journal of Chemical Engineering and Applications*, *6*(5), 376–380. https://doi.org/10.7763/IJCEA.2015.V6.513

Thaoklua, R., Janjaroen, J., & Tedsree, K. (2018). The study of activity and selectivity of calcium oxide nanocatalyst for transesterification of high free fatty acid crude palm oil. *Chiang Mai Journal of Science*, *45*(2), 973–983.

Tsai, W.-T. (2013). Microstructural characterization of calcite-based powder materials prepared by planetary ball milling. *Materials*, *6*(8), 3361–3372. https://doi.org/10.3390/ma6083361

Twaiq, F. A. A., Mohamad, A. R., & Bhatia, S. (2004). Performance of composite catalysts in palm oil cracking for the production of liquid fuels and chemicals. *Fuel Processing Technology*, *85*(11), 1283–1300. https://doi.org/10.1016/j.fuproc.2003.08.003

Verdoliva, V., Saviano, M., & De Luca, S. (2019). Zeolites as acid/basic solid catalysts: Recent synthetic developments. *Catalysts*, *9*(3). https://doi.org/10.3390/catal9030248

Wang, H., Rogers, K., Zhang, H., Li, G., Pu, J., Zheng, H., Lin, H., Zheng, Y., & Ng, S. (2019). The effects of catalyst support and temperature on the hydrotreating of waste cooking oil (WCO) over CoMo sulfided catalysts. *Catalysts*, *9*(8). https://doi.org/10.3390/catal9080689

Wang, X., Fang, Q., Wang, J., Gui, K., & Thomas, H. R. (2020). Effect of CaCO3on catalytic activity of Fe-Ce/Ti catalysts for NH3-SCR reaction. *RSC Advances*, *10*(73), 44876–44883. https://doi.org/10.1039/d0ra07351b

Weber, B., Stadlbauer, E. A., Stengl, S., Hossain, M., Frank, A., Steffens, D., Schlich, E., & Schilling, G. (2012). Production of hydrocarbons from fatty acids and animal fat in the presence of water and sodium carbonate: Reactor performance and fuel properties. *Fuel*, *94*, 262–269. https://doi.org/10.1016/j.fuel.2011.08.040

Yan, S., Lu, H., & Liang, B. (2008). Supported CaO catalysts used in the transesterification of rapeseed oil for the purpose of biodiesel production. *Energy and Fuels*, *22*(1), 646–651. https://doi.org/10.1021/ef070105o

Yi, L., Liu, H., Li, S., Li, M., Wang, G., Man, G., & Yao, H. (2019). Catalytic Pyrolysis of biomass wastes over Org-CaO/Nano-ZSM-5 to produce aromatics: Influence of catalyst properties. *Bioresource Technology*, *294*(September), 122186. https://doi.org/10.1016/j.biortech.2019.122186

Yigezu, Z. D., & Muthukumar, K. (2014). Catalytic cracking of vegetable oil with metal oxides for biofuel production. *Energy Conversion and Management*, *84*, 326–333. https://doi.org/10.1016/j.enconman.2014.03.084

Zhang, Q., Cheng, K., Kang, J., Deng, W., & Wang, Y. (2014). Fischer-tropsch catalysts for the production of hydrocarbon fuels with high selectivity. *ChemSusChem*, *7*(5), 1251–1264. https://doi.org/10.1002/cssc.201300797

Zhao, X., Wei, L., Cheng, S., Huang, Y., Yu, Y., & Julson, J. (2015). Catalytic cracking of camelina oil for hydrocarbon biofuel over ZSM-5-Zn catalyst. *Fuel Processing Technology*, *139*, 117–126. https://doi.org/10.1016/j.fuproc.2015.07.033

Zheng, Z., Lei, T., Wang, J., Wei, Y., Liu, X., Yu, F., & Ji, J. (2019). Catalytic cracking of soybean oil for biofuel over γ-Al2O3/CaO composite catalyst. *Journal of the Brazilian Chemical Society*, *30*(2), 359–370. https://doi.org/10.21577/0103-5053.20180185

Zheng, Z., Wang, J., Wei, Y., Liu, X., Yu, F., & Ji, J. (2019). Effect of La-Fe/Si-MCM-41 catalysts and CaO additive on catalytic cracking of soybean oil for biofuel with low aromatics. *Journal of Analytical and Applied Pyrolysis*, *143*(18), 104693. https://doi.org/10.1016/j.jaap.2019.104693

Zhou, X., & Chen, C. (2016). Strengthening and toughening mechanisms of amorphous/amorphous nanolaminates. *International Journal of Plasticity*, *80*, 75–85. https://doi.org/10.1016/j.ijplas.2016.01.003

Zul, N. A., Ganesan, S., Hamidon, T. S., Oh, W. Da, & Hussin, M. H. (2021). A review on the utilization of calcium oxide as a base catalyst in biodiesel production. *Journal of Environmental Chemical Engineering*, *9*(4), 105741. https://doi.org/10.1016/j.jece.2021.105741